Atmos. Meas. Tech., 8, 3263–3275, 2015
www.atmos-meas-tech.net/8/3263/2015/
doi:10.5194/amt-8-3263-2015

Atmospheric Measurement Techniques
Open Access

Plume-based analysis of vehicle fleet air pollutant emissions and the contribution from high emitters

J. M. Wang[1], C.-H. Jeong[1], N. Zimmerman[1], R. M. Healy[1], D. K. Wang[2], F. Ke[2], and G. J. Evans[1]

[1]Department of Chemical Engineering and Applied Chemistry, University of Toronto, Toronto, Ontario M5S3E5, Canada
[2]Analysis and Air Quality Section, Air Quality Research Division, Environment Canada, Ottawa, Ontario K1V1C7, Canada

Correspondence to: J. M. Wang (jonm.wang@utoronto.ca)

Received: 9 December 2014 – Published in Atmos. Meas. Tech. Discuss.: 18 March 2015
Revised: 15 July 2015 – Accepted: 16 July 2015 – Published: 13 August 2015

Abstract. An automated identification and integration method has been developed for in-use vehicle emissions under real-world conditions. This technique was applied to high-time-resolution air pollutant measurements of in-use vehicle emissions performed under real-world conditions at a near-road monitoring station in Toronto, Canada, during four seasons, through month-long campaigns in 2013–2014. Based on carbon dioxide measurements, over 100 000 vehicle-related plumes were automatically identified and fuel-based emission factors for nitrogen oxides; carbon monoxide; particle number; black carbon; benzene, toluene, ethylbenzene, and xylenes (BTEX); and methanol were determined for each plume. Thus the automated identification enabled the measurement of an unprecedented number of plumes and pollutants over an extended duration. Emission factors for volatile organic compounds were also measured roadside for the first time using a proton transfer reaction time-of-flight mass spectrometer; this instrument provided the time resolution required for the plume capture technique. Mean emission factors were characteristic of the light-duty gasoline-dominated vehicle fleet present at the measurement site, with mean black carbon and particle number emission factors of $35\,\mathrm{mg\,kg\,fuel^{-1}}$ and $7.5\times10^{14}\,\#\,\mathrm{kg\,fuel^{-1}}$, respectively. The use of the plume-by-plume analysis enabled isolation of vehicle emissions, and the elucidation of co-emitted pollutants from similar vehicle types, variability of emissions across the fleet, and the relative contribution from heavy emitters. It was found that a small proportion of the fleet (< 25 %) contributed significantly to total fleet emissions: 100, 100, 81, and 77 % for black carbon, carbon monoxide, BTEX, and particle number, respectively. Emission factors of a single pollutant may help classify a vehicle as a high emitter; however, regulatory strategies to more efficiently target multi-pollutant mixtures may be better developed by considering the co-emitted pollutants as well.

1 Introduction

On-road motor vehicles are one of the largest contributors to air pollution in urban environments (Franco et al., 2013) and are thus one of the major sources underlying the estimated 3.7 million air-quality-related deaths in 2012 worldwide (WHO, 2014). Further, traffic-related air pollution is associated with cardiovascular and respiratory diseases, and lung cancer (Laden et al., 2006; Kampa and Castanas, 2008; HEI, 2010). Vehicle emissions contain a vast number of pollutants, some with toxicological relevance such as fine particulate matter ($PM_{2.5}$), ultrafine particles (UFPs, < 100 nm diameter), carbon monoxide (CO), nitrogen oxides (NO_x), and volatile organic compounds (VOCs) including their secondary transformation to tropospheric ozone and particulate matter (Seinfeld and Pandis, 2006; HEI, 2010). Other pollutants such as carbon dioxide (CO_2) and black carbon (BC) have associated negative impacts on global climate (Sims et al., 2014). A major challenge in quantifying and modelling vehicle emissions is their highly variable and evolving nature, dependent on many factors including vehicle type, age, and operating conditions such as fuel type, engine lubricating oil, wear of parts and installed emission control technologies (HEI, 2010; Franco et al., 2013). In order to better assess the impact of vehicle emissions on local and global air quality, emissions must be more consistently and representatively quantified and characterized.

To date, many approaches have been employed to quantify vehicle emissions. Emissions models (e.g., MOVES, MOBILE, EMFAC) are necessary to produce national inventories for vehicle emissions (EC, 2008; USEPA, 2013), but their accuracy and representativeness depend on emission factors (EFs) produced by engine dynamometer and real-world emissions studies (Gertler, 2005; Franco et al., 2013). Although engine dynamometer studies provide highly accurate measurements of tailpipe emissions in controlled laboratory conditions, they have two main limitations: (1) not being fully representative of real-world emissions (e.g., driving behaviour, ambient effects on emissions pre- and post-tailpipe, wear and age of vehicles in the in-use fleet) and (2) small vehicle sample size resulting from the restrictive cost and duration of experiments (Dallmann and Harley, 2010). Real-world measurement of in-use vehicle emissions presents a suitable method to bridge the gap between laboratory and ambient observations.

Real-world studies can include on-road and tailpipe measurements that provide representative EFs for in-use vehicles (Franco et al., 2013). Similar to engine laboratory studies, these measurements typically sample a limited number of vehicles. In contrast, the measurements of vehicle emissions at the roadside or near-road region provide a much larger vehicle sample size over a relatively short period of time and have been successfully applied to tunnel (Pierson and Brachaczek, 1982; Miguel et al., 1998; Rogak et al., 1998; Kirchstetter et al., 1999; Hwa et al., 2002; Kristensson et al., 2004; Geller et al., 2005; Ban-Weiss et al., 2009; Ho et al., 2009; Dallmann et al., 2012; Mancilla and Mendoza, 2012; May et al., 2013), roadside (Bishop and Stedman, 1996; Sadler et al., 1996; Jimenez et al., 2000; Chan et al., 2004; Ko and Cho, 2006; Guo et al., 2007; Westerdahl et al., 2009; Phuleria et al., 2007), and near-road environments (Nickel et al., 2013; Liggio et al., 2012; Imhof et al., 2005; Ning et al., 2008; Ježek et al., 2014; Janhall et al., 2012). Near-road measurements can be made long-term in a range of environments that are more representative of outdoor and street-level conditions typical of human exposure points. The former measurements have further usefulness with the increasing need and implementation of near-road monitoring sites as part of regulatory action (Evans et al., 2011; Weinstock et al., 2013). Further these measurements incorporate short timescale changes that may occur between the tailpipe and near-road region for certain pollutants. However, near-road measurements have certain disadvantages as compared to tunnel and roadside measurements; higher dilution rates, increased influence from local meteorology, and less controlled conditions all affect the accuracy of the resulting EFs. Thus, it is important that near-road measurements be accompanied by site and measurement validation. Recent advancements in instrument technology, including higher-time-resolution and sensitivity measurements, have enabled improved interpretation and isolation of vehicle emissions from near-road measurements. However, such high-time-resolution measurements result in a much larger data set for processing.

This study presents an automated method for the identification, isolation, and integration of vehicle plumes from near-road pollutant measurements in an urban street canyon. Vehicle emissions quantification and characterization are presented as real-world EFs calculated from high-time-resolution measurements. Emissions were automatically identified using an algorithm developed to identify passing vehicle plumes based on changes in the measured CO_2 mixing ratio. This approach is different from previous near-road EF studies which have used up- and downwind measurements to isolate the traffic signal or have used lower-time-resolution measurements, integrating the traffic signal to calculate an overall EF for the fleet. Some studies have taken advantage of 0.5–1 Hz time resolution to isolate individual exhaust plumes from vehicles (Dallmann et al., 2012; Ban-Weiss et al., 2009; Bishop et al., 2011; Ježek et al., 2014).

A novelty of automating the plume identification technique is that a large number of plumes can be identified and captured. By maximizing the sampling size, more vehicles can be represented by the measurements, which is useful when assessing the heterogeneity of emissions and calculating the fleet EFs. Although method validation for site-specific conditions requires initial testing, data processing can be completed on the order of minutes, removing the time limitation of processing large data sets. In this study, the technique was validated for differences in manual versus automated identification and integration; dilution effects; and sensitivity analysis of the method in order to test the repeatability of the calculated EFs. Comparison with previous study EF values is used to evaluate this methodology as well as potential differences in fleet EFs. This study also presents high-time-resolution measurements of VOCs using a proton transfer reaction time-of-flight mass spectrometer (PTR-TOF-MS). While the PTR-TOF-MS has been deployed in the near-road environment (DeWitt et al., 2015), a novelty in this study is the application of this instrument to individual plume EF measurements. Three applications of the automated plume-by-plume approach are examined: (1) separation of individual plumes based on co-emitted pollutants, (2) estimation of the relative contributions of higher emitting vehicles to the overall emissions detected at the site, and (3) evaluation of local emissions regulation program.

2 Experimental methods

2.1 Measurement site

Continuous measurements were made over four campaigns, each lasting at least 4 weeks, at the Southern Ontario Centre for Atmospheric Aerosol Research (SOCAAR) Field Measurement Facility in downtown Toronto, Canada (Fig. 1): 7 November–7 December 2013 (fall), 15 February–25 March

2014 (winter), 23 April–27 May 2014 (spring), and 22 July–8 September 2014 (summer). The sampling site (43°39′32″ N, 79°23′43″ W) is located north of a four-lane major arterial roadway that experiences traffic volumes ranging from 16 000 to 25 000 vehicles per day with vehicle speeds up to 50 km h^{-1}. Located west of the sampling site is a set of traffic lights, which results in various driving states such as cruising, braking, idling, and acceleration. Stop-and-go traffic dominates during rush hour periods, while free-flowing traffic is more typical outside of these hours, especially overnight. Given the downtown location and the absence of on-road parking, there is expected to be little, if any, influence of cold start emissions. The site is a quasi-street canyon with two four-story buildings on either side of the roadway and has been used previously in urban air quality studies (Jeong et al., 2011; Rehbein et al., 2011; Sabaliauskas et al., 2012). During the measurement periods, the average hourly ambient temperature and relative humidity ranged from −18 to +31 °C and 18 to 94 %, respectively.

From the 2009 Canadian Vehicle Survey conducted by Statistics Canada, the age breakdown averaged across all on-road vehicle types in Ontario is 45 % below 5 years, 35 % 5–11 years, 14 % 12–18 years, and 6 % older than 19 years: with a mean fleet age of around 7 years (StatsCan, 2010). Based on vehicle weight class, vehicles less than 4500 kg (i.e., cars, station wagons, vans, pickup trucks, small trucks) make up 97 % of the vehicle fleet, with the remaining 3 % being trucks heavier than 4500 kg (i.e., large pickup trucks, larger trucks, tractor trailers). Of the < 4500 kg vehicle weight class, fuel type is dominated by gasoline (97 %) compared to diesel (3 %); the inverse is reported for the heavier weight class with 83 % diesel and 17 % gasoline usage (StatsCan, 2010). A similar fleet makeup is observed at the measurement site between vehicle classes (Fig. 1c, d) with roughly 3–4 % of the passing vehicles identified as trucks, with vehicle counting done using a dual radar system described in the next section.

2.2 Measurement techniques

Ambient air was continuously drawn through inlets located 15 m from the roadway and 3 m above the ground. Gaseous pollutants were drawn through approximately 2 m of 0.953 cm Teflon fluorinated ethylene propylene (FEP) tubing with a six-port glass manifold for flow distribution to gas analyzers. Measurements were made using two identical chemiluminescence analyzers, one for NO and one for NO_x, a gas filter correlation infrared analyzer for CO, and a non-dispersive infrared analyzer for CO_2 (42i, 48C, and 410i, respectively; Thermo Scientific, Waltham, MA) (Table 1). The time resolution for NO, NO_x, and CO_2 measurements was 1 s, and for CO measurements it was 10 s.

A dedicated separate 0.635 m Teflon FEP line was used for VOC sampling. A proton transfer reaction time-of-flight mass spectrometer (PTR-TOF-MS, model 8000, IONICON Analytik, Innsbruck, Austria) was connected to the line upstream of a pump providing additional flow to reduce residence time in the sampling line. The PTR-TOF-MS was operated similarly to Jordan et al. (2009) with H_3O^+ as the reagent ion, a mass range up to m/z 452, and at 2 s time resolution (Jordan et al., 2009). Individual VOCs were calibrated using two standard mixtures made by the National Air Pollution Surveillance Network at Environment Canada based on United States Environmental Protection Agency (US EPA) TO15 for 159 non-polar VOC and 40 independently chosen polar VOCs. Data were processed using PTR-MS Viewer 3.1.0.20 and converted from counts per second to mass concentration using the corresponding six-level calibration curve. In this study, the focus was the VOCs with the most distinct signal from vehicle plumes, including methanol (CH_3OH), benzene (C_6H_6), toluene (C_7H_8), and ethylbenzene + xylenes (C_8H_{10}).

For the particle-phase pollutant measurements, a 10 cm stainless steel tube inlet with a 2.5 µm cut-off was used to draw ambient air at 170 L min^{-1} with minimal particle losses in the ultrafine size range. Measurements were made using a photoacoustic soot spectrometer for particle absorption at 781 nm (PASS-3, Droplet Measurement Techniques, Boulder, CO) and a condensation particle counter for total particle number (PN) concentration (CPC, model 651, Teledyne Advanced Pollution Instrumentation, San Diego, CA), which has a particle size cut of 7 nm (Table 1). Particle absorption measurements were converted to mass concentration by linear correlation with coincident 2 h integrated measurements made with a thermal–optical organic carbon–elemental carbon analyzer (Sunset Lab OC-EC, Sunset Laboratories, Inc., Tigard, OR) (Jeong et al., 2004). The calculated conversion factor from absorption (Mm^{-1}) to mass concentration (µg m^{-3}) was 0.31, 0.27, 0.26, and 0.27 g m^{-2} for fall, winter, spring, and summer, respectively, and is specific to the study conditions and instrumentation. The PASS-3 and CPC were run at a 2 s time resolution.

Supplementary measurements including local temperature, relative humidity, and wind speed and direction were carried out using a meteorological station (WXT520, Vaisala, Vantaa, Finland) at the local site. Vehicle counts were measured by a SmartSensor HD (SS-125, Wavetronix, Provo, UT) dual radar system and categorized as light-duty (1.5–7 m) or heavy-duty vehicles (7–18 m) based on the detected approximate length. Further information on the instrumental calibration, quality assurance, and measurement techniques is provided in the Supplement.

2.3 Data analysis

Measurement data were processed and analyzed using Igor Pro 6.34. All pollutant measurement data were first time corrected to match with the CO_2 signal. This was done by a sensitivity analysis that involved shifting the time series of each pollutant in 1 s increments within a ±30 s range. Each

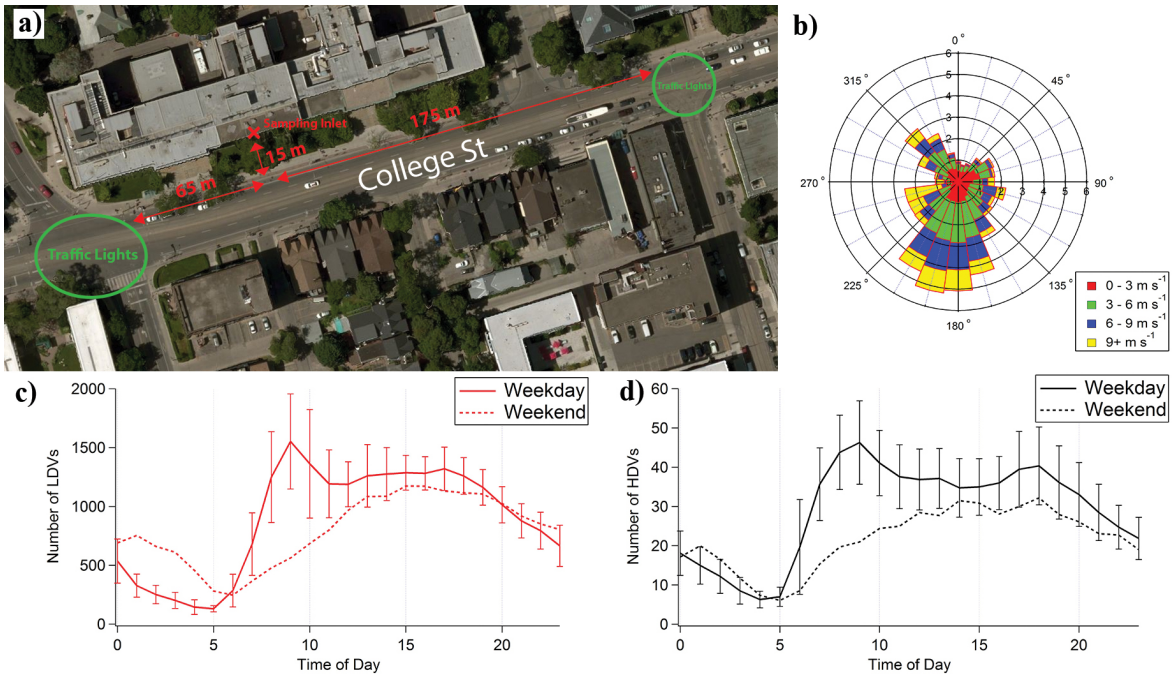

Figure 1. Aerial view of measurement site including distances between sampling inlet, roadway, and nearby traffic lights **(a)**; wind rose plot from measurements over all four campaigns **(b)**; diurnal trends of number of light-duty vehicles (LDVs) **(c)** and heavy-duty vehicles (HDVs) **(d)** with error bars indicating standard deviation. Satellite and aerial imagery is courtesy of Bing Maps.

Table 1. Summary of measurement site instrumentation and the corresponding sensitivity, range, precision and time resolution.

Parameter	Instrument type	Model	Effective sensitivity	Range (precision)[a]	Time resolution (s)
CO_2	Non-dispersive infrared gas analyzer	410i	5 ppmv	0–1000 ppmv (±1 %)	1
CO	Filter correlation infrared gas analyzer	48C	150 ppbv	0–10 ppmv (±0.1 ppmv)	10
NO NO_x	Chemiluminescence analyzer	42i	3 ppbv	0–500 ppbv (±0.4 ppbv)	1
Particle number	Condensation particle counter[b]	651	1500 # cm^{-3}	0–10^6 # cm^{-3} (±10 %)	2
Particle absorption	Photoacoustic soot spectrometer	PASS-3	8 Mm^{-1}	0–100 000 Mm^{-1} (±3.0 Mm^{-1})	2
VOCs	PTR-TOF-MS	8000	0.2–1 ppbv[c]	10 pptv–1 ppmv (±0.1 ppbv)	2

[a] Instrumental precision provided by manufacturer specifications except for PTR-TOF-MS, which was unavailable, alternative precision was calculated as 3σ from measurement of zero air, [b] particle size range of 7–2500 nm, [c] effective sensitivity range for BTEX.

time-shifted series was then correlated with the CO_2 time series to find the most appropriate lag time. After each pollutant time series was corrected for lag, typically by 0 to 10 s, it was also visually inspected to ensure the plumes matched well temporally. An algorithm was written to automatically identify vehicle exhaust plumes based on the inflection points before and after a plume calculated from the slope of the CO_2 signal averaged over 10 data points (Fig. 2). Measured plumes shorter than 10 s or with an average response over the integration period below an effective integration sensitivity of 5 ppmv s^{-1} CO_2 ($\sim$ 2 mg C m^{-3} s^{-1}) were considered erroneous or uncaptured. The capture of vehicle plumes was visually verified for selected periods over the measurement campaign for quality control of the automated identification algorithm and the defined effective sensitivity for the CO_2 signal. A fuel-based carbon balance method was used to calculate EFs (Eq. 1), similar to previous studies (Hansen and Rosen, 1990; Kirchstetter et al., 1999; Ban-Weiss et al.,

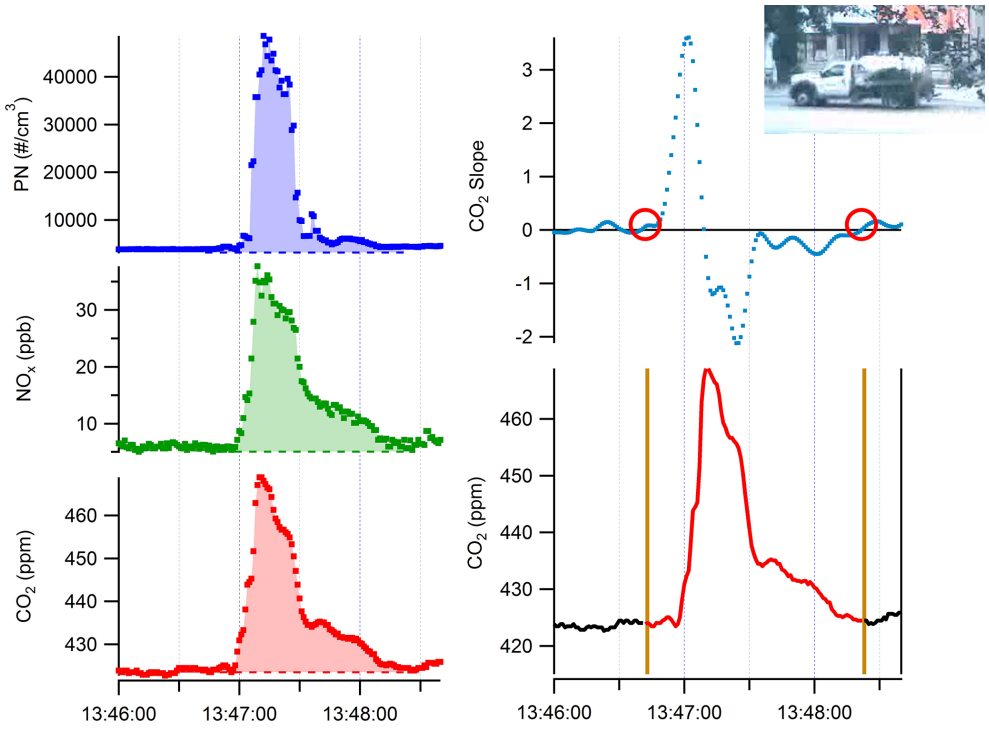

Figure 2. Time series of CO_2, NO_x, and particle number concentration from a vehicle plume (left). The slope of CO_2 and the automated identification of the plume (right) with vertical lines marking the beginning and end of the plume period. Video footage (top right) of a utility truck was associated with the identified plume.

2010; Dallmann et al., 2012),

$$\mathrm{EF}_P = \left(\frac{\Delta[P]}{\Delta[\mathrm{CO_2}] + \Delta[\mathrm{CO}]}\right) w_\mathrm{C}, \quad (1)$$

where EF_P is the fuel-based emission factor of pollutant P (in g or particle number) per kg of fuel burned at ambient conditions (i.e., 25 °C, 101.325 kPa) represented by the background-subtracted integrated amount of carbon combustion products ΔCO_2 and ΔCO (in kg of C m^{-3}), and $w_c = 0.86$ the carbon weight fraction for a gasoline-dominated fleet (Ban-Weiss et al., 2010). This background level is determined as the minimum level at the beginning or end of the plume period. For CO, the response time of the instrument is much lower than all the other instruments with plumes visibly wider than the other traces (Fig. S1 in the Supplement). Thus for CO the plume identification had to be altered slightly where the same identification algorithm was applied to identify each plume, but CO_2 was averaged to 60 s to match with the CO signal. The plume identified at this lower time resolution was then matched with the nearest plume identified using CO_2 at 1 Hz (Fig. S2). This was only required for calculating EFs for the CO signal, which was measured at a lower time response than other pollutants.

$$\text{Effective sensitivity} = \overline{(P_\mathrm{max} - P_\mathrm{min})} \quad (2)$$

$$\mathrm{EF}_\mathrm{min} = \left(\frac{\text{Effective sensitivity}}{\Delta[\mathrm{CO_2}] + \Delta[\mathrm{CO}]}\right) w_\mathrm{c} \quad (3)$$

The effective sensitivity for each instrument was determined based on period of stable signal with no vehicle influence across all measurements over 2–3 min. Three of these periods within each measurement campaign were chosen from the beginning, middle, and end of the campaign. The mean difference between the maximum and minimum signal during these stable periods (Eq. 2), corresponding to roughly 5–6σ, was used to set a minimum threshold for the plume capture criterion for each pollutant measurement (Table 1). Emission factors were calculated from captured plumes – those that had detectable CO_2 but pollutant signals lower than the instrument sensitivity were classified as below threshold (BT) EFs and calculated using the effective sensitivity value (Eq. 3). In order to calculate the fleet mean EF for a given pollutant, the BT EFs were included in calculating the mean and were either (1) set as zero or (2) calculated using Eq. (3). This constrained the possible fleet mean by giving a lower and upper limit based on the sensitivity of the instrumentation (Fig. 3). Further information on the data analysis techniques and validation is provided in the Supplement.

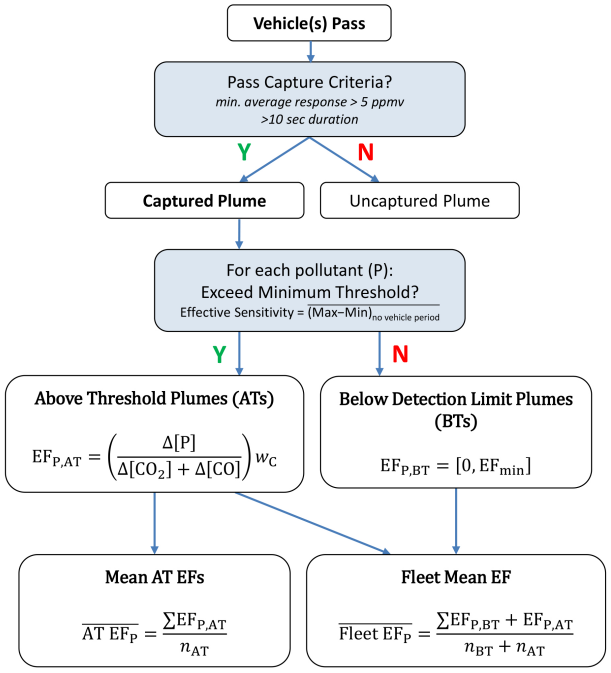

Figure 3. Process flow diagram of plume identification and capture criteria for AT and BT EFs, and the calculation for mean AT and mean fleet EFs.

A sensitivity analysis was conducted on the effects of changing various capture criteria (i.e., minimum plume duration and CO_2 response, shifting start and end times of the plumes) and is summarized in the Table S1 in the Supplement. The largest changes are −10 % for the mean CO EF when decreasing the minimum CO_2 response threshold. Benzene (C_6H_6) EFs were also impacted by changing in the minimum CO_2 response, with a change of up to −8 % with increasing response threshold. A change in minimum plume duration had little effect, mainly due to the overlap with the minimum CO_2 response criterion being more stringent than minimum plume time. However, in the extreme cases where the minimum CO_2 response threshold was set to zero to nullify its effect, changing the minimum plume time to 30 s resulted in higher values on average for the pollutant EFs. By lowering the minimum plume time to 1 s, the opposite effect is observed, mainly due to the inclusion of very small plumes having zero EF values. Neither of these criteria would ever be set for a 1 Hz CO_2 signal, as a minimum of 30 s removes nearly 70 % of the plumes whereas a minimum of 1 s would consider even the smallest increase in the CO_2 trace to be a plume.

Considering the plume start and end times, increasing or decreasing the plume period by 4 s results in a change in mean EF values of 0.2–10 %, depending on the pollutant, which is further described in the Supplement (Table S1). Increasing or decreasing the plume period by 10 s results in a change in mean EF values of 0.2–18 %, again depending on the pollutant (Table S1). However, in both cases, BT or zero EFs can affect the mean EF as a result of the minimum criterion used. Thus, a better way to look at the effects on the absolute values of EFs would be to focus on above threshold (AT) EFs only. In this case, increasing/decreasing the plume periods by 4 and 10 s results in only a 0.2–8 % and 0.2–10 % difference in mean EFs, respectively. The effect on mean EF as a function of random subsampling of the data set was also tested. With a subset containing 10 % of the original data set, the percent difference of the mean EFs ranged between 0.3 and 6.3 % depending on the pollutant with the highest being for CH_3OH. At a 1 and 0.1 % fraction of the data, the mean EFs deviated upwards of 20 and 90 %, respectively. Further discussion of the sensitivity analyses is included in the Supplement.

3 Results and discussion

3.1 Plume capture and validation

After applying plume capture criteria on the measurements, 103 000 plumes were considered captured, based on the measured CO_2, out of 153 000 automatically identified plumes (67 % captured). These plumes represented emissions from a single or at times multiple vehicles due to the large volume of vehicles on the roadway. The length of the plumes ranged from 10 to 197 s, with a mean and median duration of 57 and 53 s, respectively. In stagnant conditions, plumes have been observed to last upwards of 3 min; however these plumes are infrequent and make up less than 0.1 % of the total captured plumes. The mean and median (range) of $\Delta[CO_2]$ were 10 and 7 ppmv (3–330 ppmv), the integrated amount was 192 and 128 mg C m^{-3} s^{-1} (50–3675 mg C m^{-3} s^{-1}), and the dilution ratio calculated by assuming 140 000 ppmv (14 %) tailpipe emission of CO_2 was 15 500 and 14 000 (424–49 970). An important difference between the EFs calculated from measurements made in this quasi-street canyon compared to controlled laboratory conditions is the potential chemical or physical changes that occur for certain pollutants between emission at the tailpipe and measurement at the site (i.e., NO, NO_2, VOCs, UFPs). This is a caveat of ambient near-road measurements that are more representative of real-world conditions. A major assumption made using this technique is that dilution and transport are similar for CO_2 and all the pollutants between emission and measurement, or between the pollutants themselves when pollutant ratios are considered. Site and measurement validation was conducted by two methods: (1) coincident measurements at different distances to calculate EFs and (2) use of a test vehicle to drive by the measurement site multiple times.

To test the effects of dilution and transport on the pollutants prior to detection, coincident measurements were made for PN and CO_2 at 3 m (roadside) and 15 m (measurement inlet) distances from the roadside. Emission factors were cal-

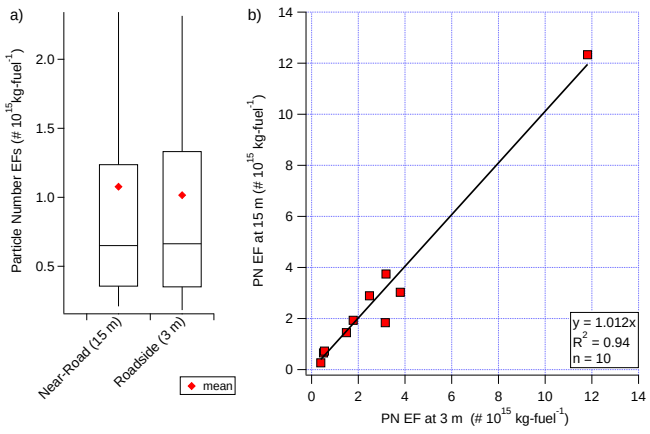

Figure 4. Particle number emission factors comparison between coincident roadside (3 m) measurements and the near-road inlet (15 m), including all captured plumes ($n = 282$) from the test period **(a)** and individual plumes ($n = 10$) from the same vehicles **(b)**. Horizontal lines represent the median values, boxes represent the 75th percentile and whiskers represent the 90th percentile.

culated on four different days based on 282 plumes from passing vehicles. The mean PN EFs differed between the independent measurements at 3 and 15 m on average by only 6 % (Fig. 4a). Individual plumes were also matched based on specific vehicles observed at the site, where the same test was conducted at night during low traffic periods where the plume travelling from the roadway could be directly associated with the plume that reach near-road building inlet. In this case, for 10 unique plumes, the average ratio of the PN EF from the two locations was 1.012 ± 0.253 % ($R^2 = 0.94$). Thus on average, EFs for these pollutants do not vary significantly in this near-road region.

During the same nighttime tests, a passenger car was driven past the measurement site multiple times in order to better test the capture efficiency of the method. The capture efficiency in this context represents the number of plumes that passed the capture efficiency divided by the total number of passes recorded from the tests. Based on CO_2 plumes that passed the minimum capture criterion, for roadside versus near-road inlet measurements, the capture efficiency at night averaged 70 and 46 %, respectively. Driving state was also investigated, where the vehicle cruised pass, was set to idle in line with, braking at, or accelerating from the inlet. Idling in line with the measurement inlet resulted in a slightly higher capture efficiency of 52 % compared to cruise, accelerating, and braking (44 %).

Individual plumes that had elevated pollutant concentrations were selected from the measurement campaign in order to link individual plumes to specific vehicles, and visually identify information on the vehicle type. These plumes were not necessarily always from a high or heavy emitter, as dilution also played a critical role in determining the measured concentrations at the inlet. These individual plumes were then classified as having no truck influence (cars only) or having at least one truck (trucks with or without cars) using video recordings of the passing vehicles. Of the 152 plumes examined, 88 had an influence from trucks, and 62 were from cars-only periods. Truck-influenced periods had higher NO_x, BC, and PN EFs on average, whereas car plumes had higher CO and BTEX (benzene, toluene, ethylbenzene, and xylene) EFs (Fig. 5). The co-emission of these pollutant sets from similar vehicle types and fuel types corresponds to previous studies (e.g., May et al. 2014).

To further test the automated identification and EF calculation algorithm, a subset of these plumes were manually identified and integrated. On average, the mean percent difference between manual and automatic methods was 8 % (Supplement) and within acceptable limits given the differences in identification, background subtraction, and integration techniques employed between the two methods. The largest deviations in EF values between the two methods were the result of noisier measurement signals that affected the background determination, especially for BC. Although both methods were consistent in the identified start of a plume, differences in the identified plume length resulted in small deviations in EF values.

3.2 Mean emission factors

The mean pollutant EFs were calculated from the total number of captured plumes including BT plumes (Table 2) respective of the entire detectable fleet. The fleet mean EF is presented with a range to include the calculation using (1) zero values and (2) the effective sensitivity based on Eq. (3) for BT EFs, which yielded similar values. Thus, the fleet mean was relatively well constrained despite the inability to measure every pollutant in every plume. In other words, the cumulative contribution of all the clean vehicles with BT EFs was very small as compared to the rest of the fleet; these vehicles make up 23 to 81 % of the fleet, depending on the pollutant. Additionally, EFs were converted into distance-based units (i.e., g km^{-1}) assuming weighted arithmetic in-use fleet mean fuel consumption rates (Supplement). In comparison with previous studies that used fuel-based EFs (Table 2), the fleet mean EFs from this study were in the lower range for certain pollutants (e.g., NO_x, PN, BC) characteristic of the gasoline-dominated light-duty vehicle (LDV) fleet observed at the measurement site.

The fleet mean NO_x EF was similar to those reported for LDVs in previous studies and significantly lower than those reported for heavy-duty vehicles (HDVs) (Hudda et al., 2013; Dallmann et al., 2012, 2013; Hu et al., 2012; Bishop et al., 2011; Park et al., 2011). For the CO EFs, a large portion of the fleet (81 %) did not have detectable CO emissions. Inclusion of those low-emitting vehicles resulted in a fleet mean CO EF within the range of those previously reported for LDVs (Dallmann et al., 2012, 2013; Wang et al., 2009; Park et al., 2011; Hu et al., 2012; Bishop et al., 2011). Plumes

Table 2. Fleet mean EFs from this study, including percentage of BT EFs, compared with the range of LDV, HDV and fleet EFs reported from other real-world fuel-based EF studies. Emission factors in km^{-1} distance-based units in the Supplement (Table S4).

Pollutant	This study		Other studies			
	Fleet mean EFs[a] ± 95 % CI	BT EFs[b] (%)	LDV EFs	HDV EFs	Units[e]	Studies
NO_x	2.29–2.33 ± 0.02	23 %	1.9–3.8	8.9–33.4	g kg fuel^{-1}	1, 2, 3, 4, 5, 6
CO	10.0–10.3 ± 0.2	75 %	14.3–55.1	7.7–10.9	g kg fuel^{-1}	1, 2, 5, 7, 8, 9
PN[c]	7.53–7.57[d] ±0.11	30 %	4–18	23–110	10^{14} # kg fuel^{-1}	2, 5, 6, 10, 11
BC[e]	35–55 ± 1	66 %	1–150	350–780	mg kg fuel^{-1}	2, 3, 12, 13, 14
	VOCs				Fleet	
CH_3OH	1.70–1.71 ± 0.08	40 %	N/A		g kg fuel^{-1}	15, 16, 17, 18, 19
C_6H_6	50–52 ± 1	49 %	23–850		mg kg fuel^{-1}	
C_7H_8	143–148 ± 6	54 %	39–1580		mg kg fuel^{-1}	
C_8H_{10}	129–135 ± 2	55 %	58–1590		mg kg fuel^{-1}	

[1] Dallmann et al. (2012), [2] Park et al. (2011), [3] Hudda et al. (2013), [4] Dallmann et al. (2013), [5] Hu et al. (2012), [6] Wang et al. (2010), [7] Wang et al. (2009), [8] Dallmann et al. (2013), [9] Bishop et al. (2011), [10] Kalafut-Pettibone et al. (2011), [11] USEPA (2008b), [12] Geller et al. (2005), [13] Westerdahl et al. (2009), [14] Liggio et al. (2012), [15] Kristensson et al. (2004), [16] Gentner et al. (2013), [17] Araizaga et al. (2013), [18] Hwa et al. (2002), [19] Ho et al. (2009)
[a] The range in the mean EFs for all identified plumes with the lower value based on BT EFs as zero and upper value calculated with the effective sensitivity,
[b] percentage of EFs treated as BT and given a zero value,
[c] particle size range of 7–2500 nm,
[d] range for fleet mean PN EFs is small due to the low effective sensitivity value of the CPC,
[e] BC EFs from the PASS-3 only had 75 % data coverage temporally due to automatic zeroing of the instrument.

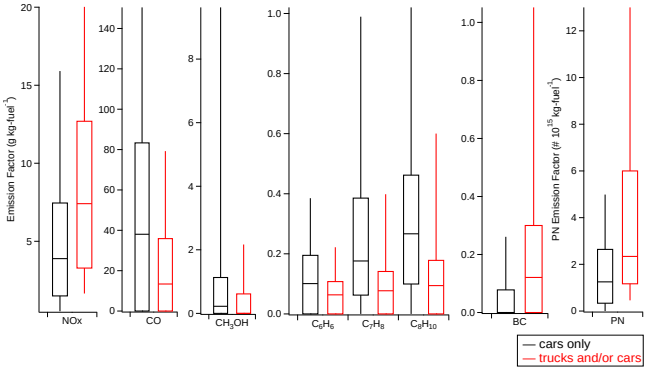

Figure 5. Box and whisker plot of the emission factors for individual plume analysis separated between periods with no influence from trucks (red) and periods with at least one passing truck (black). Horizontal lines represent the median values, boxes represent the 75th percentile and whiskers represent the 90th percentile.

containing detectable CO were not as frequently observed relative to other pollutants like NO_x. The fleet mean EFs estimated by the US EPA are a good comparison for emission model results, which for NO_x are 3.4 and 7.1 g kg fuel^{-1}, and for CO are 46 and 2 g kg^{-1} for LDVs and HDVs, respectively (USEPA, 2008a, b). In comparison with US EPA LDV CO EFs, the fleet mean CO EF in this study was lower by a factor of 4.6. If zero-value BT EFs are removed from calculating the mean the resulting mean CO EF is 39.9 g kg fuel^{-1}, which is within the upper range of LDV CO EFs previously reported and more in line with US EPA CO EFs. This implies that large discrepancies may arise between models that use the US EPA CO EFs as compared to "full fleet" real-world values, such as those determined for the fleet in this study. In contrast, the US EPA fleet mean NO_x EF for LDVs is quite comparable to the fleet mean EF calculated from this study with only a 39 % difference.

The fleet mean PN EF in this study is closer to the range of EFs reported for LDVs than for HDVs; however, there is large inter-study variability for PN EFs depending on many factors such as site and driving conditions, and measurement technique (Kalafut-Pettibone et al., 2011; Hudda et al., 2013; Park et al., 2011; Wang et al., 2010; Geller et al., 2005). The fleet mean BC EF is at the lower end of the range reported in other studies for LDVs and well below those for HDVs (Geller et al., 2005; Westerdahl et al., 2009; Park et al., 2011; Hudda et al., 2013; Dallmann et al., 2013; Liggio et al., 2012). Similar to PN EFs reported from previous studies, there is considerable inter-study variability in previously reported BC EFs, which in part may be due to the assumed mass absorption cross-section values used to convert optical to mass measurements. The BTEX mean EFs were at the lower end of those previously reported (Gentner et al., 2013; Kristensson et al., 2004; Araizaga et al., 2013; Hwa et al., 2002; Ho et al., 2009), but they are comparable to BTEX EFs reported by Gentner et al. (2013) and Araizaga et al. (2013). Unfortunately, there are no nationwide US or Canadian fleet mean EFs for PN, BC, or speciated BTEX available for comparison; thus the EF values reported here arguably represent the most up-to-date comprehensive reference point for emission of these pollutants, at least for the Canadian vehicle fleet.

3.3 Distribution of emission factors

The EFs from the measurable fleet are highly skewed and follow a lognormal distribution. This has been observed previously in vehicle emissions measurements (Stephens, 1994; Lawson et al., 1990; Bishop et al., 1996; Jimenez et al., 2000; Barth et al., 1999; Wenzel et al., 2000; Schwartz, 2000) and more recently in real-world EF studies (Kuhns et al., 2004; Bishop et al., 2011; Dallmann et al., 2012; Hudda et al., 2013). This arises because the majority of the fleet is characterized by relatively low emissions while the small portion of older poorly tuned vehicles have disproportionately high emissions. The associations between specific vehicle model year and type with this distribution have been extensively studied in the past; however, this study aims to directly quantify this skewed distribution from measurements of the passing vehicle fleet.

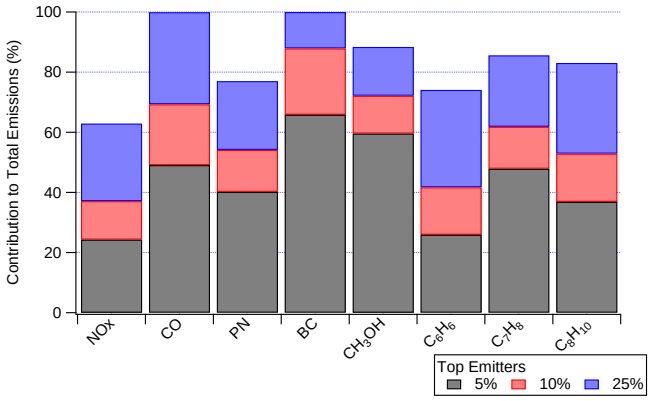

Figure 6. Stacked bar plot showing the contribution of the top 5, 10, and 25 % heaviest emitters to the total emissions captured through the plume analysis.

3.3.1 Total emissions associated with the top emitters

Although it is known that the lognormal distribution of vehicle emissions is typically the result of a small number of older poorly tuned vehicles that emit disproportionately compared to the fleet, it is important to quantify this effect within the local vehicle fleet. The percent contribution of emissions categorized from the top 5, 10, and 25 % of emitters was calculated for each pollutant (Fig. 6). For CO, BC, CH_3OH, and C_7H_8, the top 5 % of emitters contributed more than 40 % of the emissions and were the most disproportionately emitted of all the measured pollutants. In contrast, NO_x and C_6H_6 exhibited a lower contribution from the top emitters, although over 50 % of the emissions still came from 25 % of the vehicles. Specifically, for CO and BC, 25 % of vehicles produced greater than 90 % of the emissions while for CH_3OH, BTEX, and PN, 25 % of vehicles produced greater than 70 %. The number of vehicles that contributed to a single detectable plume varied; thus strictly speaking Fig. 6 represents a summary of detectable exhaust plumes rather than individual vehicles. Furthermore, the BT EFs used to calculate the percent contributions were given a zero value and this might arguably have inflated the calculated contribution from high emitters. This effect was explored by using the effective sensitivity value to calculate the BT EFs rather than using a zero value, which yielded similar distributions for all pollutants with the exception of BC (Supplement).

3.3.2 Evaluation of local emissions regulations

Vehicle emissions in southern Ontario are regulated by the provincial government through "Drive Clean", an emissions testing program that targets in-use light-duty vehicles whose emissions exceed US EPA Tier 1 limits (McCarter, 2012; MoE, 2010). The objective of the Drive Clean program is to remove high-emitting vehicles; however, it is not indicative of vehicle fleet emissions as vehicles manufactured post-2007 meet US EPA Tier 2 emission standards. Emissions testing is required every 2 years on vehicles manufactured after 1988 and older than 7 years. Further information on the emissions testing program can be found in the Supplement. A rough conversion of the maximum emissions allowed by Drive Clean for a mid-sized passenger vehicle to fuel-based EFs gives 6.5 and 44 g kg fuel^{-1} for NO_x and CO, respectively (MoE, 2010), and can be used as a reference point for evaluating the overall compliance of the fleet with the emissions testing program. From the plume-by-plume analysis, EFs from higher emitters and their contribution to the total emissions were determined.

Focusing on regulated gaseous pollutants, fleet mean EF values for NO_x and CO (Table 2) were substantially lower than the limits set by Drive Clean, with only 6 % of the EFs exceeding the limits for both pollutants. Thus, by far the majority of the vehicles complied with this emission standard. However, this small proportion of the fleet contributed 26 % for NO_x and 54 % for CO of the total fleet emissions based on EF product distributions (Fig. 7). Therefore, a disproportionately small number of vehicles contribute significantly to fleet emissions for NO_x and CO in Toronto. This disproportionality is further illustrated by the percentage of BT EF plumes of each pollutant (Table 2), where much of the CO, BC, and BTEX are emitted by a small proportion of the fleet. By querying for those plumes that are characterized by the highest NO_x emission factors, the magnitude of emissions of other pollutant species for the same vehicles can also be determined. This contribution for other pollutants can then be matched for those vehicles that exceeded the NO_x and CO limits. For example, the 6 % of high NO_x EF plumes that exceeded the Drive Clean limit also contribute 20 % of PN, 14 % of BC, 7 % of CO, and 8 % BTEX emissions (Fig. 7a). In contrast, plumes exceeding the Drive Clean CO limit had slightly higher contributions of BTEX (12 %) but relatively lower contributions of the other pollutants (Fig. 7b). This reiterates the findings from this individual plume analysis, indi-

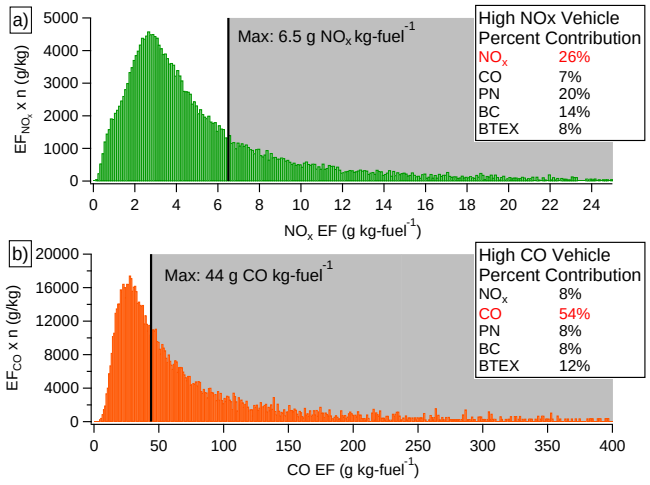

Figure 7. Product distribution histograms of NO_x **(a)** and CO **(b)** EFs of captured plumes from the detectable fleet with the maximum allowable emissions indicated by the black line. The plumes that exceed this limit (gray area) with corresponding percent contributions of other pollutants (text box). Not shown are 28 and 67 % of BT EF plumes for NO_x and CO, respectively.

cating that more stringent enforcing of CO limits may have a co-benefit in decreasing BTEX; however targeting high NO_x emitting vehicles would decrease PN and BC more significantly.

A disproportionate contribution of NO_x and CO emission from a small number of vehicle plumes indicates the effectiveness of local emissions regulation as well as good infiltration of new well-tuned vehicles into the vehicle fleet; however, there is room for improvement in terms of removal of the higher emitters. Previous studies have benefited greatly from single vehicle information and have shown trends in EFs with increasing model year (Jimenez et al., 2000; Kuhns et al., 2004; Bishop et al., 2011; Wenzel et al., 2000). Although this study only had limited visual information for identifying individual vehicles, capturing a high sample size of plumes allowed both for the quantification of the fleet distribution of emissions and the investigation of relationships between pollutants. It is important to note that this comparison with the Drive Clean limits is approximate as it includes HDVs, which follow different standards and various driving states including stop-and-go and acceleration that may result in higher emissions of pollutants (Barth et al., 1999; Kuhns et al., 2004; Bishop and Stedman, 2008; Kean et al., 2003). The impact of stop-and-go traffic on real-world emissions is increased in urban environments where traffic lights and high-density traffic dominate; therefore, it is important to include variable driving conditions in real-world analyses. Additionally, some of these "higher emitting" vehicles may not be high emitters under cruise conditions and as Drive Clean only tests at steady-state cruise speeds, these vehicles may potentially pass emissions testing.

4 Summary and conclusions

In this study an automated plume identification algorithm and emission factor calculation was validated and applied to near-road measurements in Toronto, Ontario. The analysis includes 4 months of measurements over a wide range of environmental conditions and provides an updated snapshot of emissions from the local vehicle fleet. With a growing number of near-road monitoring networks being implemented, similar methods can be employed with pre-existing sites and instrumentation allowing for long-term measurements to isolate and quantify vehicle emissions. The automation of the plume identification coupled with high-time-resolution measurements greatly improves the sample size and quality of the EF data in this study. Despite not capturing every passing vehicle, the high number of plumes sampled allowed for an in-depth analysis and characterization of emissions from a representative variety of vehicles. This complex information would otherwise be difficult to separate from time-integrated measurements of fleet emissions. The approach also allows for the direct quantification of the distribution of fleet emissions and a broad evaluation of the effectiveness of local emissions regulations on the in-use fleet in real-world operation. An advantage of the plume-by-plume approach is the time resolution it provides, where samples time integrated over hours would likely result in mean EFs much lower than those of the high emitters, and not allow estimation of the impact of these high emitters. This information can also be combined, on a plume-by-plume basis, to determine the contribution from a subset of higher emitting vehicles to unregulated pollutants (e.g., BC and PN) in relation to current emissions standards. Given the large data set from the four measurement campaigns, temporal and seasonal analyses of the EFs will be conducted in a future publication. Additionally, this study presents PTR-TOF-MS measurements of BTEX and CH_3OH from vehicle exhaust in the near-road environment, representing a novel application of this technique. These compounds were included as marker of VOCs from vehicle exhaust for the method validation; however, mass spectral data have been retained for each plume and will be used in future much more detailed analyses to characterize volatile organics from various vehicle types.

The Supplement related to this article is available online at doi:10.5194/amt-8-3263-2015-supplement.

Acknowledgements. This study was undertaken with financial support of the Government of Canada through the federal Department of the Environment and operational support from the Ontario Ministry of the Environment. Infrastructure support was provided by the Canada Foundation for Innovation and the Ontario Research Fund. Additional instrumentation, associated calibration

standards, and analysis support were provided by the National Air Pollution Surveillance Network, Environment Canada. Specific technical support for the PTR-TOF-MS was provided by Stefan Feil from IONICON Analytik. Robert M. Healy's contribution was funded by the Marie Curie Action FP7-PEOPLE-IOF-2011 (project: CHEMBC, no. 299755).

Edited by: S. Malinowski

References

Araizaga, A. E., Mancilla, Y., and Mendoza, A.: Volatile Organic Compound Emissions from Light-Duty Vehicles in Monterrey, Mexico: a Tunnel Study, Int. J. Environ. Res., 7, 277–292, 2013.

Ban-Weiss, G. A., Lunden, M. M., Kirchstetter, T. W., and Harley, R. A.: Measurement of Black Carbon and Particle Number Emission Factors from Individual Heavy-Duty Trucks, Environ. Sci. Technol., 43, 1419–1424, doi:10.1021/es8021039, 2009.

Ban-Weiss, G. A., Lunden, M. M., Kirchstetter, T. W., and Harley, R. A.: Size-resolved particle number and volume emission factors for on-road gasoline and diesel motor vehicles, J. Aerosol Sci., 41, 5–12, doi:10.1016/j.jaerosci.2009.08.001, 2010.

Barth, M., An, F., Younglove, T., Levine, C., Socora, G., Ross, M., and Wenzel, T.: Development of a Comprehensive Modal Emissions Model – Final Report NCHRP Project 25-11, Transportation Research Board – National Research Council, Washington DC, 1–214, 1999.

Bishop, G. A. and Stedman, D. H.: Measuring the emissions of passing cars, Acc. Chem. Res., 29, 489–495, 1996.

Bishop, G. A., Stedman, D. H., and Ashbaugh, L.: Motor Vehicle Emissions Variability, J. Air. Waste Manage., 46, 667–675, doi:10.1080/10473289.1996.10467501, 1996.

Bishop, G. A. and Stedman, D. H.: A Decade of On-road Emissions Measurements, Environ. Sci. Technol., 42, 1651–1656, doi:10.1021/es702413b, 2008.

Bishop, G. A., Schuchmann, B. G., Stedman, D. H., and Lawson, D. R.: Emission Changes Resulting from the San Pedro Bay, California Ports Truck Retirement Program, Environ. Sci. Technol., 46, 551–558, doi:10.1021/es202392g, 2011.

Chan, T. L., Ning, Z., Leung, C. W., Cheung, C. S., Hung, W. T., and Dong, G.: On-road remote sensing of petrol vehicle emissions measurement and emission factors estimation in Hong Kong, Atmos. Environ., 38, 2055–2066, doi:10.1016/j.atmosenv.2004.01.031, 2004.

Dallmann, T. R. and Harley, R. A.: Evaluation of mobile source emission trends in the United States, J. Geophys. Res.-Atmos., 115, D14305, doi:10.1029/2010JD013862, 2010.

Dallmann, T. R., DeMartini, S. J., Kirchstetter, T. W., Herndon, S. C., Onasch, T. B., Wood, E. C., and Harley, R. A.: On-Road Measurement of Gas and Particle Phase Pollutant Emission Factors for Individual Heavy-Duty Diesel Trucks, Environ. Sci. Technol., 46, 8511–8518, doi:10.1021/es301936c, 2012.

Dallmann, T. R., Kirchstetter, T. W., DeMartini, S. J., and Harley, R. A.: Quantifying On-Road Emissions from Gasoline-Powered Motor Vehicles: Accounting for the Presence of Medium- and Heavy-Duty Diesel Trucks, Environ. Sci. Technol., 47, 13873–13881, doi:10.1021/es402875u, 2013.

DeWitt, H. L., Hellebust, S., Temime-Roussel, B., Ravier, S., Polo, L., Jacob, V., Buisson, C., Charron, A., André, M., Pasquier, A., Besombes, J. L., Jaffrezo, J. L., Wortham, H., and Marchand, N.: Near-highway aerosol and gas-phase measurements in a high-diesel environment, Atmos. Chem. Phys., 15, 4373–4387, doi:10.5194/acp-15-4373-2015, 2015.

EC: Uncertainty Analysis of Criteria Air Contaminants from Mobile Sources in Canada, Environment Canada, Ottawa, Canada, 1–4, 2008.

Evans, G. J., Jeong, C.-H., Sabaliauskas, K., Jadidian, P., Aldersley, S., Larocque, H., and Herod, D.: Design of a Near-Road Monitoring Strategy for Canada, A Final Report to Environment Canada, SOCAAR, Toronto, 1–60, 2011.

Franco, V., Kousoulidou, M., Muntean, M., Ntziachristos, L., Hausberger, S., and Dilara, P.: Road vehicle emission factors development: A review, Atmos. Environ., 70, 84–97, doi:10.1016/j.atmosenv.2013.01.006, 2013.

Geller, M. D., Sardar, S. B., Phuleria, H., Fine, P. M., and Sioutas, C.: Measurements of Particle Number and Mass Concentrations and Size Distributions in a Tunnel Environment, Environ. Sci. Technol., 39, 8653–8663, doi:10.1021/es050360s, 2005.

Gentner, D. R., Worton, D. R., Isaacman, G., Davis, L. C., Dallmann, T. R., Wood, E. C., Herndon, S. C., Goldstein, A. H., and Harley, R. A.: Chemical Composition of Gas-Phase Organic Carbon Emissions from Motor Vehicles and Implications for Ozone Production, Environ. Sci. Technol., 47, 11837–11848, doi:10.1021/es401470e, 2013.

Gertler, A. W.: Diesel vs. gasoline emissions: Does PM from diesel or gasoline vehicles dominate in the US?, Atmos. Environ., 39, 2349–2355, doi:10.1016/j.atmosenv.2004.05.065, 2005.

Guo, H., Zhang, Q., Shi, Y., and Wang, D.: On-road remote sensing measurements and fuel-based motor vehicle emission inventory in Hangzhou, China, Atmos. Environ., 41, 3095–3107, doi:10.1016/j.atmosenv.2006.11.045, 2007.

Hansen, A. D. A. and Rosen, H.: Individual Measurements of the Emission Factor of Aerosol Black Carbon in Automobile Plumes, J. Air. Waste Manage., 40, 1654–1657, doi:10.1080/10473289.1990.10466812, 1990.

HEI: Traffic-Related Air Pollution: A Critical Review of the Literature on Emissions, Exposure, and Health Effects Health Effects Institute, Boston, 1–108, 2010.

Ho, K. F., Lee, S. C., Ho, W. K., Blake, D. R., Cheng, Y., Li, Y. S., Ho, S. S. H., Fung, K., Louie, P. K. K., and Park, D.: Vehicular emission of volatile organic compounds (VOCs) from a tunnel study in Hong Kong, Atmos. Chem. Phys., 9, 7491–7504, doi:10.5194/acp-9-7491-2009, 2009.

Hu, J., Wu, Y., Wang, Z., Li, Z., Zhou, Y., Wang, H., Bao, X., and Hao, J.: Real-world fuel efficiency and exhaust emissions of light-duty diesel vehicles and their correlation with road conditions, J. Environ. Sci., 24, 865–874, doi:10.1016/S1001-0742(11)60878-4, 2012.

Hudda, N., Fruin, S., Delfino, R. J., and Sioutas, C.: Efficient determination of vehicle emission factors by fuel use category using on-road measurements: downward trends on Los Angeles freight corridor I-710, Atmos. Chem. Phys., 13, 347–357, doi:10.5194/acp-13-347-2013, 2013.

Hwa, M.-Y., Hsieh, C.-C., Wu, T.-C., and Chang, L.-F. W.: Real-world vehicle emissions and VOCs profile in the Taipei tunnel

located at Taiwan Taipei area, Atmos. Environ., 36, 1993–2002, doi:10.1016/S1352-2310(02)00148-6, 2002.

Imhof, D., Weingartner, E., Ordóñez, C., Gehrig, R., Hill, M., Buchmann, B., and Baltensperger, U.: Real-World Emission Factors of Fine and Ultrafine Aerosol Particles for Different Traffic Situations in Switzerland, Environ. Sci. Technol., 39, 8341–8350, doi:10.1021/es048925s, 2005.

Janhall, S., Molnar, P., and Hallquist, M.: Traffic emission factors of ultrafine particles: effects from ambient air, J. Environ. Monit., 14, 2488–2496, doi:10.1039/C2EM30235G, 2012.

Jeong, C.-H., Hopke, P. K., Kim, E., and Lee, D.-W.: The comparison between thermal-optical transmittance elemental carbon and Aethalometer black carbon measured at multiple monitoring sites, Atmos. Environ., 38, 5193–5204, doi:10.1016/j.atmosenv.2004.02.065, 2004.

Jeong, C.-H., McGuire, M. L., Godri, K. J., Slowik, J. G., Rehbein, P. J. G., and Evans, G. J.: Quantification of aerosol chemical composition using continuous single particle measurements, Atmos. Chem. Phys., 11, 7027–7044, doi:10.5194/acp-11-7027-2011, 2011.

Ježek, I., Drinovec, L., Ferrero, L., Carriero, M., and Mocnik, G.: Determination of car on-road black carbon and particle number emission factors and comparison between mobile and stationary measurements, Atmos. Meas. Tech. Discuss., 7, 5423–5455, doi:10.5194/amtd-7-5423-2014, 2014.

Jimenez, J. L., McManus, J. B., Shorter, J. H., Nelson, D. D., Zahniser, M. S., Koplow, M., McRae, G. J., and Kolb, C. E.: Cross road and mobile tunable infrared laser measurements of nitrous oxide emissions from motor vehicles, Chemosphere – Global Change Science, 2, 397–412, doi:10.1016/S1465-9972(00)00019-2, 2000.

Jordan, A., Haidacher, S., Hanel, G., Hartungen, E., Märk, L., Seehauser, H., Schottkowsky, R., Sulzer, P., and Märk, T. D.: A high resolution and high sensitivity proton-transfer-reaction time-of-flight mass spectrometer (PTR-TOF-MS), Int. J. Mass Spectrom., 286, 122–128, doi:10.1016/j.ijms.2009.07.005, 2009.

Kalafut-Pettibone, A. J., Wang, J., Eichinger, W. E., Clarke, A., Vay, S. A., Blake, D. R., and Stanier, C. O.: Size-resolved aerosol emission factors and new particle formation/growth activity occurring in Mexico City during the MILAGRO 2006 Campaign, Atmos. Chem. Phys., 11, 8861–8881, doi:10.5194/acp-11-8861-2011, 2011.

Kampa, M. and Castanas, E.: Human health effects of air pollution, Environ. Pollut., 151, 362–367, doi:10.1016/j.envpol.2007.06.012, 2008.

Kean, A. J., Harley, R. A., and Kendall, G. R.: Effects of Vehicle Speed and Engine Load on Motor Vehicle Emissions, Environ. Sci. Technol., 37, 3739–3746, doi:10.1021/es0263588, 2003.

Kirchstetter, T. W., Harley, R. A., Kreisberg, N. M., Stolzenburg, M. R., and Hering, S. V.: On-road measurement of fine particle and nitrogen oxide emissions from light- and heavy-duty motor vehicles, Atmos. Environ., 33, 2955–2968, doi:10.1016/S1352-2310(99)00089-8, 1999.

Ko, Y.-W. and Cho, C.-H.: Characterization of large fleets of vehicle exhaust emissions in middle Taiwan by remote sensing, Sci. Total Environ., 354, 75–82, doi:10.1016/j.scitotenv.2005.05.040, 2006.

Kristensson, A., Johansson, C., Westerholm, R., Swietlicki, E., Gidhagen, L., Wideqvist, U., and Vesely, V.: Real-world traffic emission factors of gases and particles measured in a road tunnel in Stockholm, Sweden, Atmos. Environ., 38, 657–673, doi:10.1016/j.atmosenv.2003.10.030, 2004.

Kuhns, H. D., Mazzoleni, C., Moosmüller, H., Nikolic, D., Keislar, R. E., Barber, P. W., Li, Z., Etyemezian, V., and Watson, J. G.: Remote sensing of PM, NO, CO and HC emission factors for on-road gasoline and diesel engine vehicles in Las Vegas, NV, Sci. Total Environ., 322, 123–137, doi:10.1016/j.scitotenv.2003.09.013, 2004.

Laden, F., Schwartz, J., Speizer, F. E., and Dockery, D. W.: Reduction in Fine Particulate Air Pollution and Mortality, American Journal of Respiratory and Critical Care Medicine, 173, 667–672, doi:10.1164/rccm.200503-443OC, 2006.

Lawson, D. R., Groblicki, P. J., Stedman, D. H., Bishop, G. A., and Guenther, P. L.: Emissions from lit-use Motor Vehicles in Los Angeles: A Pilot Study of Remote Sensing and the Inspection and Maintenance Program, J. Air. Waste Manage., 40, 1096–1105, doi:10.1080/10473289.1990.10466754, 1990.

Liggio, J., Gordon, M., Smallwood, G., Li, S.-M., Stroud, C., Staebler, R., Lu, G., Lee, P., Taylor, B., and Brook, J. R.: Are Emissions of Black Carbon from Gasoline Vehicles Underestimated? Insights from Near and On-Road Measurements, Environ. Sci. Technol., 46, 4819–4828, doi:10.1021/es2033845, 2012.

Mancilla, Y. and Mendoza, A.: A tunnel study to characterize $PM_{2.5}$ emissions from gasoline-powered vehicles in Monterrey, Mexico, Atmos. Environ., 59, 449–460, doi:10.1016/j.atmosenv.2012.05.025, 2012.

May, A. A., Presto, A. A., Hennigan, C. J., Nguyen, N. T., Gordon, T. D., and Robinson, A. L.: Gas-particle partitioning of primary organic aerosol emissions: (1) Gasoline vehicle exhaust, Atmos. Environ., 77, 128–139, doi:10.1016/j.atmosenv.2013.04.060, 2013.

May, A. A., Nguyen, N. T., Presto, A. A., Gordon, T. D., Lipsky, E. M., Karve, M., Gutierrez, A., Robertson, W. H., Zhang, M., Brandow, C., Chang, O., Chen, S., Cicero-Fernandez, P., Dinkins, L., Fuentes, M., Huang, S.-M., Ling, R., Long, J., Maddox, C., Massetti, J., McCauley, E., Miguel, A., Na, K., Ong, R., Pang, Y., Rieger, P., Sax, T., Truong, T., Vo, T., Chattopadhyay, S., Maldonado, H., Maricq, M. M., and Robinson, A. L.: Gas- and particle-phase primary emissions from in-use, on-road gasoline and diesel vehicles, Atmos. Environ., 88, 247–260, doi:10.1016/j.atmosenv.2014.01.046, 2014.

McCarter, J.: 2012 Annual Report, Office of the Auditor General of Ontario, Toronto, Canada, 107–128, 2012.

Miguel, A. H., Kirchstetter, T. W., Harley, R. A., and Hering, S. V.: On-Road Emissions of Particulate Polycyclic Aromatic Hydrocarbons and Black Carbon from Gasoline and Diesel Vehicles, Environ. Sci. Technol., 32, 450–455, doi:10.1021/es970566w, 1998.

MoE: Drive Clean Guide – Emissions Standards, Emission Test Methods, and Technical Information Relating to Ontario Regulation 361/98 As Amended, Ontario Ministry of the Environment, Toronto, Ontario, 1–20, 2010.

Nickel, C., Kaminski, H., Bellack, B., Quass, U., John, A., Klemm, O., and Kuhlbusch, T. A. J.: Size Resolved Particle Number Emission Factors of Motorway Traffic Differentiated between Heavy and Light Duty Vehicles, Aerosol Air Qual. Res., 13, 450–461, 2013.

Ning, Z., Polidori, A., Schauer, J. J., and Sioutas, C.: Emission factors of PM species based on freeway measurements and comparison with tunnel and dynamometer studies, Atmos. Environ., 42, 3099–3114, doi:10.1016/j.atmosenv.2007.12.039, 2008.

Park, S. S., Kozawa, K., Fruin, S., Mara, S., Hsu, Y.-K., Jakober, C., Winer, A., and Herner, J.: Emission Factors for High-Emitting Vehicles Based on On-Road Measurements of Individual Vehicle Exhaust with a Mobile Measurement Platform, J. Air. Waste Manage., 61, 1046–1056, doi:10.1080/10473289.2011.595981, 2011.

Phuleria, H. C., Sheesley, R. J., Schauer, J. J., Fine, P. M., and Sioutas, C.: Roadside measurements of size-segregated particulate organic compounds near gasoline and diesel-dominated freeways in Los Angeles, CA, Atmos. Environ., 41, 4653–4671, doi:10.1016/j.atmosenv.2007.03.031, 2007.

Pierson, W. R. and Brachaczek, W. W.: Particulate Matter Associated with Vehicles on the Road. II, Aerosol Sci. Technol., 2, 1–40, doi:10.1080/02786828308958610, 1982.

Rehbein, P. J. G., Jeong, C.-H., McGuire, M. L., and Evans, G. J.: Strategies to Enhance the Interpretation of Single-Particle Ambient Aerosol Data, Aerosol Sci. Technol., 46, 584–595, doi:10.1080/02786826.2011.650334, 2011.

Rogak, S. N., Pott, U., Dann, T., and Wang, D.: Gaseous Emissions from Vehicles in a Traffic Tunnel in Vancouver, British Columbia, J. Air. Waste Manage., 48, 604–615, doi:10.1080/10473289.1998.10463713, 1998.

Sabaliauskas, K., Jeong, C.-H., Yao, X., Jun, Y.-S., Jadidian, P., and Evans, G. J.: Five-year roadside measurements of ultrafine particles in a major Canadian city, Atmos. Environ., 49, 245–256, doi:10.1016/j.atmosenv.2011.11.052, 2012.

Sadler, L., Jenkins, N., Legassick, W., and Sokhi, R. S.: Remote sensing of vehicle emissions on British urban roads, Sci. Total Environ., 189–190, 155–160, doi:10.1016/0048-9697(96)05204-7, 1996.

Schwartz, J.: Smog Check II Evaluation – Part II: Overview of Vehicle Emissions, California Inspection and Maintenance Review Committee, Sacramento, California, 1–72, 2000.

Seinfeld, J. H. and Pandis, S. N.: Organic Atmospheric Aerosols, in: Atmospheric Chemistry and Physics: From Air Pollution to Climate Change, John Wiley & Sons Inc., Hoboken, New Jersey, 628–657, 2006.

Sims, R., Schaeffer, R., Creutzig, F., Cruz-Núñez, X., D'Agosto, M., Dimitriu, D., Meza, M. J. F., Fulton, L., Kobayashi, S., Lah, O., McKinnon, A., Newman, P., Ouyang, M., Schauer, J. J., Sperling, D., and Tiwari, G.: Transporation, Intergovernmental Panel on Climate Change, Cambridge, United Kingdom, 599–670, 2014.

StatsCan: Canadian Vehicle Survey: Annual 2009, Statistics Canada, Ottawa, Ontario, 1–41, 2010.

Stephens, R. D.: Remote Sensing Data and a Potential Model of Vehicle Exhaust Emissions, J. Air. Waste Manage., 44, 1284–1294, 1994.

USEPA: Average In-Use Emissions from Heavy-Duty Trucks, United States Environmental Protection Agency, Washington DC, United States, 6, 1–6, 2008a.

USEPA: Average Annual Emissions and Fuel Consumption for Gasoline-Fueled Passenger Cars and Light Trucks, United States Environmental Protection Agency, Washington DC, United States, 6, 1–6, 2008b.

USEPA: Technical Support Document, Preparation of Emissions Inventories for the Version 6.0, 2011 Emissions Modeling Platform, US Environmental Protection Agency, Washington DC, United States, 1–146, 2013.

Wang, F., Ketzel, M., Ellermann, T., Wåhlin, P., Jensen, S. S., Fang, D., and Massling, A.: Particle number, particle mass and NO_x emission factors at a highway and an urban street in Copenhagen, Atmos. Chem. Phys., 10, 2745–2764, doi:10.5194/acp-10-2745-2010, 2010.

Wang, X., Westerdahl, D., Chen, L. C., Wu, Y., Hao, J., Pan, X., Guo, X., and Zhang, K. M.: Evaluating the air quality impacts of the 2008 Beijing Olympic Games: On-road emission factors and black carbon profiles, Atmos. Environ., 43, 4535–4543, doi:10.1016/j.atmosenv.2009.06.054, 2009.

Weinstock, L., Watkins, N., Wayland, R., and Baldauf, R.: EPA's Emerging Near-Road Ambient Monitoring Network: A Progress Report, Air & Waste Management Association, Pittsburg, Pennsylvania, 6–10, 2013.

Wenzel, T., Singer, B. C., and Slott, R.: Some Issues in the Statistical Analysis of Vehicle Emissions, Journal of Transportation and Statistics, 3, 1–14, 2000.

Westerdahl, D., Wang, X., Pan, X., and Zhang, K. M.: Characterization of on-road vehicle emission factors and microenvironmental air quality in Beijing, China, Atmos. Environ., 43, 697–705, doi:10.1016/j.atmosenv.2008.09.042, 2009.

WHO: 7 million premature deaths annually linked to air pollution, World Health Organization, Geneva, Switzerland, 2014.